Synthesis, characterization and bio-evaluation of core-shell QDs with ZnSe, CdS and CdSe combinations

Sreenu Bhanoth[1], Anuraj Kshirsagar[1], Pawan K Khanna[1*], Aakriti Tyagi[2], Ankita Leekha[2], Vijay Kumar[2], Anita Verma[2*]

[1]*Quantum Dots R & D Lab, Department of Applied Chemistry, Defence Institute of Advanced Technology (DIAT), Ministry of Defence, Govt. of India, Girinagar, Pune 411021, India*
[2]*Nano Bio-Tech Lab, Department of Zoology, Kirorimal College, University of Delhi, Delhi*

[*]Corresponding author, E-mail: pawankhanna2002@yahoo.co.in, akamra23@hotmail.com

Received: 29 February 2016, Revised: 10 May 2016 and Accepted: 25 August 2016

DOI: 10.5185/amlett.2017.6495
www.vbripress.com/aml

Abstract

Present article describes one-pot, two-stage, *in-situ* controlled atmosphere method for synthesis of core-shell quantum dots (QDs) comprising of ZnSe, CdS and CdSe combinations e.g. CdS/CdSe, ZnSe/CdS and ZnSe/CdSe. The present method emphasizes on creating an effective surface passivation of core as well as formation of passivated shell *via* utilization of cyclo-octeno-1, 2, 3-selenadiazole as a precursor for selenium. Synthesis of ZnSe/CdS was compared by using two different selenium precursors *viz* cyclo-octeno-1, 2, 3-selenadiazole (C8-SDZ) and cyclo-hexeno-1, 2, 3-selenadiazole (C6-SDZ). Optical properties (UV-Visible and PL spectroscopy) indicate narrow peak width with band gap ranging in between 2.30 eV to 2.56 eV. The XRD analysis revealed the formation of respective core-shell QDs with zinc blende crystal structure. TEM analysis showed formation of spherical shaped core-shell QDs with lattice spacing of 0.35 nm due to presence of (111) crystal plane. By virtue of the excellent optical properties of ZnSe/CdS core shell QDs, this was subjected to bio-evaluation in terms of cytotoxicity and therapeutic efficacy. Approximately, 65% bio-toxicity was observed in MCF-7 with negligible haemolysis by ZnSe/CdS QDs. About, 34% tumour regression was shown by ZnSe/CdS QDs, as against 93% observed by Mitomycin C (Positive control) with respect to placebo (PBS). Copyright © 2017 VBRI Press.

Keywords: Core-shell QDs, selenadiazole, cytotoxicity.

Introduction

Over the last three decades, the scope of research in the field of quantum dots (QDs) has attracted scientists globally due to wide-ranging applications [**1**] e.g. their direct utility in QDs sensitized solar cell (QDSSC), bio-medical, LEDs and in environmental science [**2**]. Amongst various types of QDs derived from group III-V, II-VI, II-IV, II-III-VI etc. metal chalcogenide QDs comprising of group 12-16 elements of the periodic table e.g. sulphide, selenide and tellurides of zinc and cadmium in particular, have been studied extensively [**3**]. The major interest in this class of material has been mainly due to their tunable optical properties which can be altered by controlling particle size, morphology and composition of nano-crystals. Such tiny particles are often unstable upon isolation and require additional surface improvements. The *in-situ* synthesis of quantum dots using suitable long chain organic molecules with functionalities like amine, phosphines or carboxylates have been demonstrated as an excellent growth and nucleation controlling chemical tools for proving stability and dispersibility to the nano-particles. Inappropriate or incompetent chemical passivation leads to compromise in quantum dots quality in terms of their optical properties as well as long term stability leading to poor technological orientation. Presence of voids on the surface of QDs are responsible for the generation of traps for charge carriers (holes or electrons) and excitons resulting in reduction of the quantum yields (QYs) and photo-stability [**4**]. In order to avoid formation of the defects and to improve photo-stability as well as quantum yields of the QDs, perfect passivation is crucial [**5**]. The surface passivation can be based on organic molecules and /or inorganic materials [**6**, **7**]. As the shell thickness plays important role in determining optical properties of the core shell nano-crystals with respect to quantum yield and photo-stability, inorganic passivation allows one to further optimize the thickness of the shell with better control than organic passivation. Generally, three major types of inorganic passivation are practiced to synthesize useful core-shell nanostructures *viz*; semiconductors over metals, metal over semiconductors and semiconductor over semiconductor. Tremendous efforts have been made to synthesize various types of core/shell nano-crystals e.g. high temperature, hot

injection synthetic method operated between 200-300 °C which produces core shell QDs with very narrow size particle distribution in a variety of materials (CdS/ZnSe, CdTe/CdS, CdTe/CdSe, InP/ZnS and $CuInSe_2$/ZnS) [**8-16**]. In addition to the famous hot injection method; there are various other reports in the literature describing the synthesis of core shell QDs and their applications. Reiss *et al* presented effective surface passivation of CdSe nanocrystals by coating with higher band-gap QDs like ZnSe to attain high photo-luminescence efficiency (60-85%) and low size dispersibility [**17**]. Nizamoglu *et al.* described the use of CdSe/ZnS core-shell QDs for white light emitting diodes (WLED) wherein they have explained about the control over the energy transfer among the nano-crystals by changing the integrated number of nano-crystals on LED chip [**18**]. Organically passivated ZnSe nanoparticles were studied for their photo-physical and morphological properties by Sharma *et al.* [**19**].

Low temperature synthesis of the core-shell QDs was presented by the Fei *et al.* with optical studies [**20**]. Guo *et al.* [**21**] reported novel CdS/CdSe nano-rod arrays by chemical bath deposition of CdSe on hydrothermally synthesized CdS nanorods. Such core shell arrays showed enhancement in the visible light absorption ability as well as photocurrent performance as compared to their bare nano-crystals. Above reported methods uses toxic stabilizers or long chain polymers for size control, passivation and mono-dispersity of core-shell QDs, low use of source precursor solution and expensive autoclaves; however, mono-dispersity and size control using eco-friendly approach remains the challenge for the modern era.

II-VI QDs play an important role in biological applications due to high chemical stability and their ability to show absorptions and emission properties in the visible spectrum that can be tuned to desired wavelengths depending on the size and surfaces. Such properties are considered suitable for bio-imaging and drug delivery, thus making QDs appropriate for biological applications, in addition to their other potential applications in light emitting devices [**22-25**]. Core-shell QDs may offer added advantages due their further tunability in optical behaviour because such nano-structures have inorganic to inorganic combinations thereby making them more stable. Normally, the property of non-core shell type QDs is mainly governed by the inorganic core and its interaction with the surrounding environment of organic ligands because of surface related phenomena.

When the core-shell system mainly based on inorganic semiconductors is chosen for replacing organically capped normal QDs, the combinations of various factors may result improved optical properties e.g. a) Core QDs with the thin layers of the initial organic passivation b) Core QDs passivated effectively by inorganic shell layer and c) Core shell QDs possessing inorganic shell capped by organic surfactant. Although, QDs offer various benefits, their applications have been limited due to integral problems like heavy metal associated toxicity. Especially, presence of cadmium, lead, or zinc warrants special studies to avoid the damage to cells in culture and tissues in animals. Unless the detailed toxicological studies have been undertaken to establish the possible side effects of use of QDs *in-vivo*, it is inappropriate to consider them for application in biological systems.

Our past efforts [**26**] have resulted in successful synthesis of CdSe, ZnSe QDs and ZnSe/CdSe core-shell structures. We wish to continue our efforts to generate various combinations of similar QDs by adopting selenadiazole as precursor of selenium thus avoiding use of toxic capping agents/stabilizers such as TOP, TOPO etc. The use of cyclohexeno-1, 2, 3 -selenadiazole (C6-SDZ) as selenium precursor in the synthesis of QDs [**27**] and core shell nano-crystals have proved to be very successful and therefore, we got impulse for the synthesis of various core-shell nano-crystals using other derivatives or compounds of the selena diazoles (SDZ) and study their effect on the quality of the core-shell nano-crystals. In view of the above, present study emphasizes on use of organoselenium compound with 6- and 8-member cyclic ring for synthesis of novel core-shell nanostructures. Thus the present article describes utility of cycloocteno-1, 2, 3-selenadiazole (C8-SDZ) in particular as a novel selenium precursor for the synthesis of CdS/CdSe, ZnSe/CdS and ZnSe/CdSe core-shell QDs. The comparative study of the ZnSe/CdS core-shell QDs synthesized using cyclohexeno-1, 2, 3-selenadiazole (C6-SDZ) and C8-SDZ precursors is also presented. High fluorescence stability and possible toxicity of ZnSe/CdS core-shell QDs synthesized using C6-SDZ as selenium source impelled to study cytotoxicity. Therefore, the present article also focuses on the cytotoxicity of ZnSe/CdS core-shell QDs on EAC, MCF-7and HEK-29 anti-cancer cell lines in addition to *in-vivo* haemolysis and tumour regression.

Experimental

Materials and methods

Zinc acetate, cadmium oxide, diphenyl ether, oleic acid, ethanol, sulphur, dimethylsulphoxide (DMSO), para formaldehyde and (3-(4, 5-dimethylthiazol-2-yl)-2, 5-diphenyltetrazolium bromide were purchased from Sigma Aldrich and used without further purification. Cyclohexeno-1, 2, 3-selenadiazole (C6-SDZ) and Cycloocteno-1, 2, 3 selenadiazole (C8-SDZ) were prepared by reported method [**28**]. Powder X-ray diffraction (XRD) patterns were acquired with a Bruker D8 Advance diffractometer with CuKα radiation (1.5405 Å) at 45 kV and 40 mA. UV-Visible absorption spectra were recorded at room temperature with analyticjena SPECORD @ 210 plus spectrophotometer and photoluminescence (PL) was measured with Cary-Eclipse Fluorescence spectrophotometer of Agilent Technology by setting various excitation wavelengths. Raman spectra were recorded using EZ Raman spectrometer (Emitted wavelength is 780 nm) in the range 4000 to 400 cm^{-1}. Transmission electron microscopy (TEM) FEI Tecnai G2 with 30 KV was utilized for imaging of the QDs on carbon coated copper grids. Fluorescence microscope Nikon 90i at magnification 20x was used for imaging of cytotoxic cells.

Synthesis of CdS/CdSe core-shell QDs using C8-SDZ (A)

In a typical procedure, 0.5 g of cadmium acetate was added in a mixture of oleic acid and diphenyl ether (10 ml each), resulting mixture was then heated at 110 °C under N_2

atmosphere. The temperature of mixture was further increased up to 150 °C and sulphur powder (0.06 g) pre-dissolved in 10 ml diphenyl ether was added. The reaction mixture was stirred for another 30 min. The progress of formation of CdS was monitored by UV-Visible spectroscopy. For the growth of CdSe shell, cadmium acetate (0.7 g) and Cycloocteno-1, 2, 3 selenadiazole (0.40 g) pre-dissolve in DPE, were added in to same mixture. The stirring of the mixture was continued for another 20-30 min. The progress of the reaction was monitored by UV-Visible spectroscopy. After confirming formation of QDs by absorption spectroscopy, the reaction was terminated and the temperature was brought down to 40-45 °C. 10 ml of n-hexane was added as along with 25 ml of methanol for precipitation purpose. The mixture was kept for aging overnight. The precipitate of core-shell QDs was collected by centrifugation at 6000 rpm by repeated cycles of 30 min. So-obtained precipitate was dried at 50°C in an oven for 3-5 hours.

Synthesis of ZnSe/CdS core-shell QDs using C8-SDZ (B)

Core ZnSe nano crystals were initially prepared *via* customized literature method developed by our group [**26**]. Typically, 1.54g of Zn $(Ac)_2$ was dissolved in a mixture containing oleic acid (20 ml) and diphenyl ether (35 ml) at 120°C under N_2 atmosphere. The temperature was increased to 185 °C. Subsequently, cycloocteno-1, 2, 3-selenadiazole (1.0 g) pre-dissolved in 10 ml of diphenyl ether was added and reaction mixture was stirred for 10-15 min. For over growth of CdS shell, the temperature of the reaction mixture was brought down to 150 °C and CdO (0.674 g) along with sulphur powder (0.189 g) was added to the mixture. Rest of the method was similar to as described in procedure for (A). Finally, ZnSe/CdS QDs were collected *via* centrifugation process and dried at 60 °C in an oven for 4 hours.

Synthesis of ZnSe/CdSe core-shell QDs using C8-SDZ (C)

The procedure for synthesis of core ZnSe QDs was same as described for B and CdSe shell was grown over ZnSe as per procedure above section for A for shell growth.

Synthesis of ZnSe/CdS core shell QDs using C6-SDZ (D)

Initially core ZnSe nano crystals were prepared *via* customized literature method developed by our group [**26**] using Cyclohexeno-1, 2, 3-selenadiazole (C6-SDZ) as precursor of the selenium. The procedure for the over growth of CdS shell was same as described for B.

The *in vitro* bio-evaluation was done on Human Embryonic Kidney cell line (HEK-293) and Human breast adenocarcinoma (MCF-7) cell line (American Type Culture Collection, Rockville, MD). Confluent flasks were sub-cultured and maintained at 37 °C in Dulbecco's modified Eagle's medium (Sigma, St. Louis, MO) supplemented with 10% fetal calf serum (Himedia), and antibiotic containing 50 U/mL of penicillin (Sigma) and 50 mg/mL of streptomycin (Sigma, USA) under a humidified atmosphere (5% CO_2). Briefly, $5x10^3$ cells/well of HEK-293, MCF-7 and EAC cells were plated in 96-well microtiter plates. ZnSe/CdS QDs were then added to the cells at defined concentrations (10 µg/ml, 5 µg/ml and 2.5 µg/mL) and incubated for 24 hrs and 48 hrs. After incubation, 20µl of MTT(3-(4,5-dimethylthiazol-2-yl)-2, 5-diphenyltetrazolium bromide; (5 mg/mL) was then added per well. The plate was further incubated for four hours in an incubator. After incubation, the media was discarded carefully without disturbing the formazan crystals in the wells and 140 µl of dimethyl sulfoxide was added to solubilize the formazan crystals formed and readings were taken (Synergy HT, Biotek, USA) using a 540 nm filter [**29**]. All measurements were done in triplicates. Percentage viability of the cells was calculated as the ratio of mean absorbance of triplicate readings with respect to mean absorbance of control wells.

Cell viability = $(I_{control} - I_{sample}/I_{control}) \times 100$ (i)

Cellular uptake

For understanding the internalization of nanoparticles, cellular uptake was assessed in a fluorescence microscope as per our published protocols [**30**]. Briefly, MCF-7, HEK-29 and EAC cells were cultured on coverslips till 95% confluence was attained. The cells were further incubated with 10 µg/ml of ZnSe/CdS QDs. The cells were fixed with 4% paraformaldehyde and visualized under a fluorescence microscope Eclips 90i, Nikon at Mag.20x.

Haemolytic activity

Haemolytic activity was done on whole blood and percent haemolysis calculated as per previously published protocol [**31**]. Briefly, the heparinised blood procured from mice was washed twice with PBS (pH 7.4) prior to the assay. 100 µl of RBC were suspended in PBS at 1:1 ratio, and were incubated with ZnSe/CdS quantum dots of various concentration i.e 10 µg/ml, 5 µg/ml, and 2.5 µg/ml at 37ºC. The absorbance of the lysed RBC was read in a UV visible spectrophotometer (Biotek, USA) at 540 nm, 2 h post incubation. Percent haemolysis was calculated using the formula:

% Haemolysis = Absorbance of the sample/ Absorbance of the positive control *100 (ii)

Results and discussion

Synthesis and characterization

Under well controlled reaction conditions, the reaction of thermally unstable organoselenium compounds in presence of metal ions leads to the formation of respective metal chalcogenide QDs. The earlier successful syntheses of the QDs albeit of noncore-shell nature, have been reported by us using such organoselenium compounds as precursor for the selenium [**26**, **27**]

In our recent report we have highlighted possible double role of oleic acid (OLA) as a capping agent during synthesis of magic sized CdSe by microwave irradiation [**27**]. The reaction under thermal condition may similarly lead to the isomerisation of the oleic acid from *cis* to *trans* isomer at a temperature higher than 180 °C. It is well known that, *cis* form of the oleic acid is stereochemically stable however; at higher temperature conversion of *cis* to *trans* isomer is also possible and therefore, in presence of metal salt oleic acid facilitates the formation of *cis* and *trans* metal oleate during the course of reaction. Cycloocteno-1, 2, 3-selenadiazole (C8-SDZ) like its 6-member counterpart (C6-SDZ) is thermally labile organoselenium compound which upon thermolysis

liberates free selenium which subsequently reacts *in-situ* with metal ions like Zn^{2+}, Cd^{2+} etc. In the present case, during the synthesis of ZnSe/CdS and ZnSe/CdSe core-shell QDs initial reaction of the metal salt with oleic acid results in the formation of *cis* and *trans* metal-oleate as an intermediate similar to that has been described by one of us earlier. Further addition of SDZ in reaction mixture could possibly leads to the formation of highly unstable transition intermediate containing SDZ coordinated with the metal oleate. Such intermediates further react with the free selenium liberated from the C6-SDZ and C8-SDZ upon gentle heating leading to the formation of good quality QDs [**27-34**] *via* rapid nucleation. The restricted movement of the QDs by *cis*-oleic acid during the nucleation process shows control over shape and size of core QDs leading to very small particle size with narrow distribution probably can be called as early-stage nano-cluster(close to magic sized). However, *trans*-isomer of oleic acid (elaidic acid) shows free movement due to linear chain structure and therefore, allows QDs to grow homogeneously and thus forms rapidly grown regular QDs. The *cis* OLA capped QDs are possibly more favourable for the shell growth probably due to the more steric hindrance with restricted free movement during nucleation leading to the smaller size particles as well as easy replacement favouring inorganic shell layer formation. In case of CdS/CdSe core shell QDs, the direct reaction of the Cd^{2+} ions with free selenium results in the CdSe shell which can easily grow over the initially synthesized CdS core of the QDs. The selenadiazole based reactions for metal chalcogenide synthesis, are more straight forward for selenide core to selenide shell type of QDs however, when selenide/sulphide heterostructures are to be generated, the conduct of the experiments become more challenging. The overall pictorial mechanistic illustration for the synthesis of core shell QDs is shown in **scheme 1**. The growth of the CdSe shell over CdS and ZnSe core as well as CdS shell over ZnSe core can be easily identified by observation of drastic change in color. The change in color of the reaction mixture indicates changes in the nature of material and their surface that can be monitored and confirmed by UV-Visible spectroscopy.

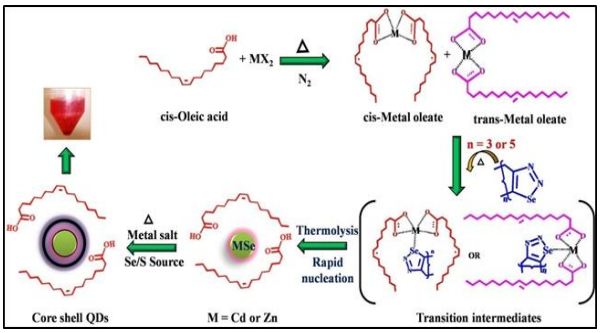

Scheme 1. Possible general mechanistic illustration of synthesis of core-shell QDs.

The reaction progress of CdS/CdSe, ZnSe/CdS and ZnSe/CdSe core shell QDs synthesized using C8-SDZ was monitored by UV-Visible spectroscopy and it was observed that, as reaction progresses the absorption value shifts towards the higher wavelength indicating the overgrowth of the shell around the core. From **Fig. 1** it can be seen that the trend is similar in all cases (inset **Fig. 1A**, **B**, **C**, **D**). After 30 min of completion of reaction absorption values for CdS/CdSe, ZnSe/CdS and ZnSe/CdSe synthesized using C8 SDZ was found to be 483 nm, 505 nm, 513 nm respectively while in case of ZnSe/CdS synthesized using C6-SDZ absorbance was near 539 nm. As the absorption, peak shifts towards red region it indicates change in particle size of the QDs due to formation of shell layer over the core.

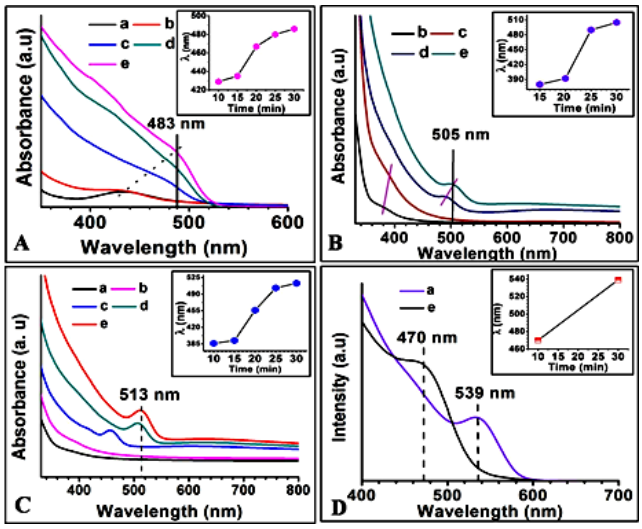

Fig. 1. Reaction progress (a=10 min, b=15 min, c= 20 min, d= 25 min, e=30 min) monitored using UV-visible spectra of 1:1 A) CdS/CdSe, B) ZnSe/CdS and C) ZnSe/CdSe synthesized using C8 and D) UV-visible spectra of 1:1 ZnSe/CdS synthesized using C6.

Table 1. Calculated band gap energies from UV-visible absorption spectrum

Reaction time	A	B	C	D
Band gap (eV) @10 min.	2.88	3.19	3.22	2.63
Band gap (eV) @30 min.	2.56	2.45	2.41	2.30

Initial absorption observed at lower wavelength is related to core quantum dots. However, the red shift obtained in each case indicating the dominance of shell. The calculated band gap values are given in **Table 1** which is further confirming the decrease in band gap with respect to the red shift for UV-visible absorption. Furthermore, the comparison of the ZnSe/CdSe core shell QDs synthesized using C6-SDZ and C8-SDZ revealed that, the synthesis using selenadiazoles with higher carbon in the ring (C8-SDZ) facilitated formation of smaller size particles however, on reduction of carbon numbers from eight to six in the ring (C6-SDZ) made adverse impact with respect to particle size and the band gap. In such study the band gap values after 30 min of reaction indicated a difference of about 0.15 eV. The photoluminescence spectra of as-synthesized core shell QDs exhibited the variation in luminescence behaviour when excited between 320-500 nm. The variation in emission properties depended on core to shell combinations (**Fig. 2**). Thus, it is established that the core and shell in such nanostructures may influence emission properties of final product. The Stokes shift of as less as 2 nm to as high as 79 nm is observed for various

samples. The smaller Stokes shift related well with the high quality of the QDs. Of the four nanostructures studied in the present case, three of them showed narrow emission shifts with respect to absorption bands. According to **Fig. 2A** the broad emission spectrum showed a band at 562 nm at an excitation wavelength of 500 nm for CdS/CdSe QDs with Stoke shift of about 79 nm. It is opined that the large Stokes shift could be due to the presence of voids or defects on the surface of the nanostructures by virtue of uncontrolled shell layer formation or dandling bonds. Inhomogeneous shell formation may possibly result due to nearly matching cation size in the core as well as shell in CdS/CdSe. Other two core shell QDs (**Fig. 2B** and **C**) synthesized using C8-SDZ being hetero-structures showed emissions at 512 and 520 nm upon excitation at 450 and 430 nm with much smaller Stokes shift (7 and 2 nm) respectively. In case of ZnSe/CdSe QDs synthesized using C6-SDZ exhibited emission at 545 nm with Stokes shift of 6 nm. The stability of the core shell QDs was tested by excitation at 320 nm, 400 nm and 450 nm. According to results, the core shell QDs synthesized using C6-SDZ was found to be very stable since at different excitations, emission wavelength was found constant (i. e. at 545 nm). The peak intensity however was suppressed upon lowering the excitation wavelength. The suppression of intensity with variation of excitation energy is a usual phenomenon in quantum dots. Also, observation of emission peak at the fixed wavelength irrespective of variation in excitation energy indicate excellent quality of the core-shell QDs. Overall the peak width of 38-43 nm was due to the homogeneous nature of the sample. The broad emission obtained in case of core shell QDs synthesized using C8-SDZ was attributed to the surface defects and the presence of vacancies in the crystal structure of core shell QDs. Such surface defects or vacancies are responsible for the low quantum yield of the core shell QDs in comparison with their respective core. Narrow peak obtained in case of the core shell QDs synthesized using C6-SDZ indicate greater phase purity and less surface defects with smaller particle size. The core ZnSe exhibited quantum yield of about 40%. However, the quantum yield of ZnSe-CdS QDs was much lower. Low quantum yield could be due to rapid layer growth of CdS shell around the ZnSe core resulting in surface defects. Overall data are presented in **Table 2**.

Table 2. Characteristic properties of core-shell ZnSe/CdS QDs

Sample	λ_{abs}(nm)	λ_{em}(nm)	Band gap (eV)	PXRD 2θ° values at different planes			Crystallite size from XRD(nm)	Particle size from TEM(nm)
				111	220	311		
ZnSe[29]	325	375	3.81	27.0	46.5	55.0	2.2	-
CdS[26]	450	455	2.75	26.0	44.0	53.4	4.9	-
CdS/CdSe (A)	483	562	2.56	25.8	43.5	50.8	2.0	4.0
ZnSe/CdS (B)	505	512	2.45	25.6	43.6	50.9	1.9	6.0
ZnSe/CdSe (C)	513	520	2.41	25.0	42.4	49.6	2.0	5.0
ZnSe/CdS (D)	539	545	2.30	25.0	42.2	50.0	2.6	3 .0

The particle size distribution of as-synthesized core shell QDs is shown in **Fig. S1**. The particle size obtained for ZnSe/CdS synthesized using C8-SDZ (curve B) was in the range of 1 to 3 nm which is much smaller than that of the same core shell QDs synthesized using C6-SDZ (5 to 10 nm, curve D). The maximum particle size with narrow particle size distribution was obtained in case of ZnSe/CdS QDs synthesized using C6-SDZ indicating more particle size homogeneity. The other two core shell QDs showed broad particle size distribution indicating various sized particle formation with maximum density distribution near 3 nm and 4 nm respectively. The narrow size distribution is mainly due to the effective passivation of core as well as shell in overall structures but could have been boosted due to the presence of inorganic shell during the reaction coupled with the umbrella of the organic surfactant.

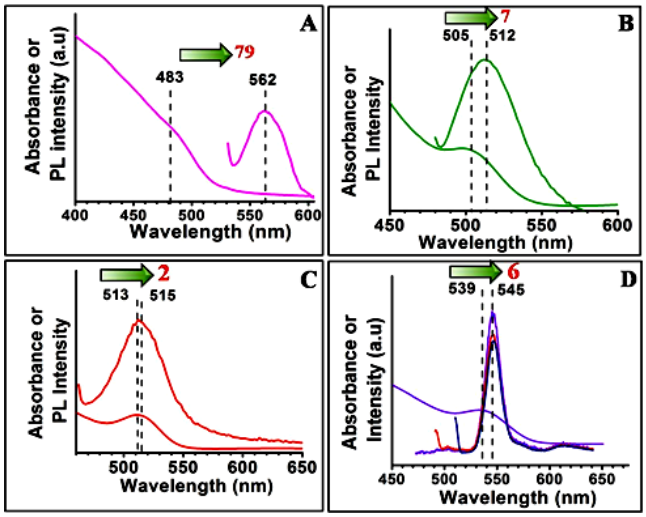

Fig. 2. Comparison of UV-Visible absorption and photoluminescence of 1:1 A) CdS/CdSe, B) ZnSe/CdS and C) ZnSe/CdSe synthesized using C8 and D) 1:1 ZnSe/CdS synthesized using C6. The red colored numbers indicating the Stokes shift.

It is important to understand the crystal structure of quantum dots before putting them to any application as the lattice arrangements may play important role in achieving useful information. XRD measurement of the samples was carried out as powders and was interpreted based on the information available in the literature. According to literature data, the Bragg's diffractions for cubic zinc blend ZnSe has characteristic features at 27.0º, 46.5º, 55.0º corresponding to (111), (220) and (311) reflection planes respectively. However, the wurtzite structure of ZnSe shows six to eight different peaks for various planes such as (100), (002), (101), (102), (110), (103) and (112) [**29**]. Similarly, XRD pattern of CdS and CdSe quantum dots showed reflections for zinc blend phase at 26.0º, 44.0º, 53.4º and 25.9º, 42.5º, 50.3º respectively corresponding to (111), (220) and (311) crystal planes and hexagonal crystal structure shows similar patterns as known for ZnSe but Bragg's reflection at different 2θ values. In the present case XRD pattern obtained for core shell QDs showed diffractions for (111), (220) and (311) crystal planes as shown in **Fig. 3** (**Table 2**). Shift in the 2θ value of the core-shell nano-structures in comparison with parent core and shell QDs confirms the formation of the shell around the core QDs.

The shift observed in case of ZnSe/CdSe synthesized using C8-SDZ was more as compared to the other core shell QDs which could be due to the difference in the thickness of the CdSe shell around ZnSe core [**17**]. The comparison of the ZnSe/CdS QDs synthesized using two different precursor showed no particular difference in the diffraction values suggesting the phase pure crystal

formation using both precursors (viz C6-SDZ and C8-SDZ). The XRD pattern obtained in all cases, clearly emphasizing on the initial formation of cubic crystal structure of the core which further gets converted to core shell retaining the same crystal structure.

Thus, 2θ values near 25.65º, 43.25º and 50.83º were observed for the core-shell QDs synthesized using C6-SDZ and C8-SDZ as precursor of selenium. The average crystallite size obtained for core shell QDs using Scherrer equation is presented in **Table 2**. The average crystallite size obtained from XRD was lower than the particle size obtained from particle size analyzer and TEM which is quite obvious. Therefore, results are in good agreement with the particle size obtained from particle size analyzer and TEM results.

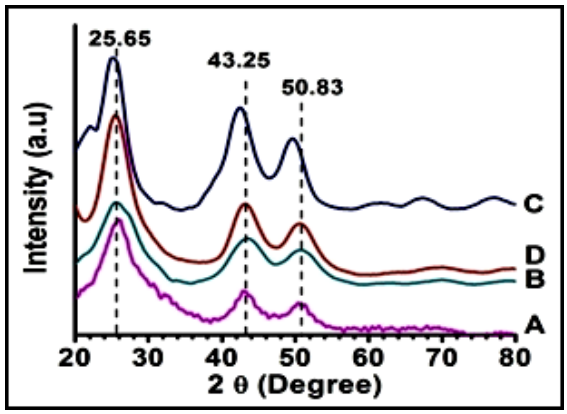

Fig. 3. XRD pattern of as-synthesized A) CdS/CdSe, B) ZnSe/CdS, C) ZnSe/CdSe using C8 as precursor and D) ZnSe/CdS synthesized using C6 as precursor.

Raman scattering observed in all cases clearly confirms the formation of the shell around the core QDs. According to the **Fig. S2** (**A**, **B**, **C**, **D**) peaks obtained near 200 cm^{-1} are assigned to transverse optical (TO), longitudinal optical (LO) and surface optical (SO) combination modes of CdS or CdSe QDs. However the intensity of peak varies depending on the shell thickness as well as the possible scattering from the core QDs [**35**]. Another Raman scattering was observed near 320 cm^{-1} because of the LO of the CdS and CdSe QDs. Important spectral features near 400 cm^{-1} revealing the presence of core shell interface interactions as well as 2LO bands of the CdSe shell in case of A and C. The possible alloy formation at the interface of core and shell and thickening of shell shows increase in the intensity near 400 cm^{-1}. The scattering observed in the range of 500-600 cm^{-1} could be assigned to the combined modes of the CdS_{SO+LO}, CdS_{alloy}, $CdS_{LO+alloy}$, $CdSe_{LO}$ and $CdSe_{LO+alloy}$. According to the literature reports, as particle size increases the full width at half maxima (FWHM) of the LO phonon peak decreases[35].The same trend is also observed here in present case. This assumption can be utilized to validate the particle size obtained from the XRD, TEM and particle size analyzer. **Table S1** shows the relation between the particle sizes obtained from TEM and calculated FWHM of the peak near 400 cm^{-1} in all cases of the core shell QDs. SEM images of so-synthesized QDs are shown in **Fig. S3**. SEM images obtained for the CdS/CdSe and ZnSe/CdS core shell QDs synthesized using C8-SDZ as selenium precursor (**Fig. S3 A**, **B**) showed very small particles of the respective core shell QDs without agglomeration. The so- synthesized QDs are too small that the particle size from the images cannot be predicted even though images were recorded at 30 nm scale bar. This indicates the core shell QDs are of very small size and nearly homogeneous forming rough surface without agglomeration. The ZnSe/CdSe QDs synthesized using C8-SDZ resulted in to small agglomerated globules with smooth surface indicating no clear separation of the QDs.

The agglomeration of QDs may be took place due to the excess capping of the QDs during the synthesis. However, this may be considered as an effect of precursor on the synthesis of ZnSe/CdSe QDs. ZnSe/CdS core shell QDs synthesized using C6-SDZ resulted in smaller particles with rough morphology. The size of these QDs is also too small and particle size from images cannot be obtained. However, comparison of images clearly reveals that the size of ZnSe/CdS core shell QDs synthesized using C6-SDZ is large when compared with the core shell QDs obtained from C8-SDZ. This trend is also evident from particle size analysis.

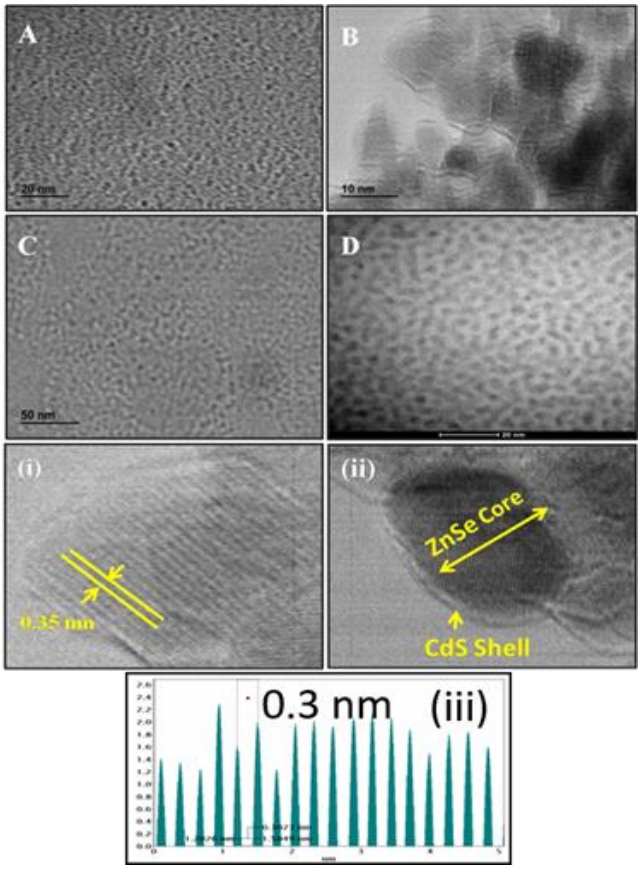

Fig. 4. TEM images of as-synthesized A) CdS/CdSe, B) ZnSe/CdS, C) ZnSe/CdSe using C8 as precursor and D) ZnSe/CdS synthesized using C6 as precursor, (i) enlarged image of B revealing interplanner distance of about 0.35 nm (ii) HRTEM image of B showing completely grown CdS shell over ZnSe core and (iii) line profile of ZnSe/CdS QDs. (The scale bar for the images A, B, C and D are 20, 10, 50 and 20 nm respectively).

Fig. 4 shows TEM images of the core shell QDs. Nearly homogeneous and monodisperse core shell QDs were obtained in all cases. **Fig. 4 A** corresponds to the CdS/CdSe core shell QDs synthesized using C8-SDZ and confirming the presence of very small particles homogeneously spread.

Lattice fringes with inter planner distance of about 0.35 nm was obtained in HRTEM image of the ZnSe/CdS (**Fig. 4B** and **(i)**) corresponding to the zinc blend crystal structure. **Fig. 4C** and **D** confirms the formation of smaller spherical particles of the ZnSe/CdSe core shell QDs synthesized using C8-SDZ and ZnSe/CdS core shell QDs synthesized using C6-SDZ respectively.

In this case also particles were homogeneously spread with nearly monodispersity. SAED pattern obtained in case of ZnSe/CdS synthesized using C6-SDZ further confirms polycrystalline zinc blend crystal structure because of diffractions due to (111), (220) and (311) crystal planes. The results obtained from TEM are in good agreement with the XRD results proving the zinc blend crystal structure and particle size (**Table 2**) of the core shell QDs. The presence of shell around core was also confirmed from the HRTEM image of ZnSe/CdS core shell QDs. According to the literature reports [**21**] the evidence for the presence of shell around the core can be revealed from HRTEM images. Here in the present case also same strategy was employed to obtain clear picture of core and shell. Therefore, image (**Fig. 4 (ii)**) taken under high resolution clearly reflecting the presence of shell layer CdS around the core of ZnSe QDs.

Biotoxicity and therapeutic evaluation

The surface chemistry, size, charge, and monodispersity of QDs are probable properties for application in various fields including biology. Utility of quantum dots in biosciences is limited due to its toxicity issues. In view of this, it is imperative to study the effect of quantum dots on human cell lines. Thus the chemically synthesized quantum dots were further evaluated for their biosuitability. In our studies ZnSe/CdS treated with MCF-7, HEK-293 and EAC cells were fixed and visualized under fluorescence microscope (Eclips 90i, Nikon **Fig. 5)**. King-Heiden *et al.*[36], have confirmed the release of free cadmium and discussed the toxicity of CdSe QDs, CdSe/ZnS QDs in the zebra fish embryo *Danio rerio*. It has been described and hypothesized that size dependent intracellular routing enables QDs to reach organelles that are otherwise unreachable to metal ions. Parak *et al.* [**37**] have proposed that following the uptake by a cell, QDs are sort of packaged into small intracellular vesicles and are transported from the cell periphery to the perinuclear region Another study suggested by Beyersmann[38] gave a contrasting opinion, whereby, it was proposed that cadmium ions are mostly located in the cytoplasm, where they are sequestered by metallothione. If QDs cause DNA mutations without cell death, then their effects maybe propagated through future generations of cells and ultimately lead to a disease.

QDs prepared by the current method by virtue of having carboxylate surface functional group, may impact the release of reactive oxygen species from internal bio system which in turn will be a useful parameter for greater understanding because higher content of oxygen species will give rise to high biotoxicity. Alternatively, it may impact the release of free metal ions. Cadmium and selenium are fundamentally toxic to cells and living systems, leading to reservation over their potential toxicity for *in vivo* applications.

In our study, core-shell ZnSe/CdS showed more cytotoxicity towards MCF-7 cell lines both post 24 hrs and 48 hrs with varied concentrations - 2.5 µg, 5 µg and 10 µg of QDs when compared to the other cell lines- HEK-293 and EAC. Around 62.77%, 28.95% and 50.02% cytotoxicity was observed subsequently in MCF-7, HEK-293 and EAC cell lines at a concentration of 10 µg in 48 hrs. 12% reduced toxocity was observed by EAC cell lines in 48 hrs, and 2% less cytotoxicity was indicated post 24 hrs in EAC, by the hydrophobic ZnSe/CdS. Our experimental studies have clearly indicated that QDs were more cytotoxic in MCF-7 than HEK-293, and EAC cells. Biotoxicity was maximumally evident at 48 hrs incubation time at a concentration of 10 µg QDs in MCF-7 cell lines. After performing several experiments, we observed that cytotoxicity, cellular uptake, internalization are both concentration and time dependent as evident in figure 8. The cytotoxicity of QDs related to their physicochemical states were observed by Bruchez *et al.* [**39**]. We observed that the major toxicity of QDs was dependent on the release of metal ions (e.g., Cd^{2+}) which is in agreement with the published literature reports [**40**, **41**]. Haemolysis of QDs was performed on blood procured from healthy mice using PBS (pH 7.4). 10 µg/ml and 2.5 µg/ml of ZnSe/CdS exhibited ~1.74% haemolysis followed by 5µg/ml that showed low haemolysis (~1.5%) in 2 h. The low percent of haemolysis gave the confidence that the QDs were biocompatible and could be used for *in vivo* studies (**Fig. 9**).

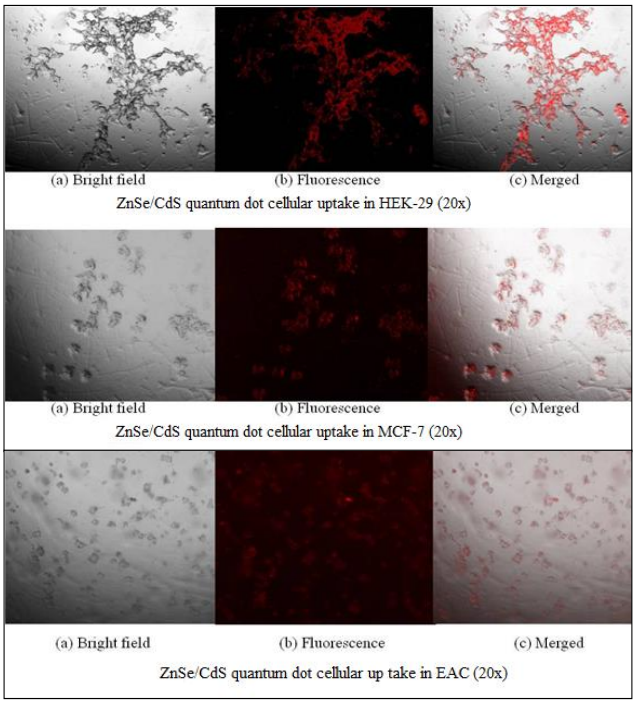

Fig. 5. Cellular uptake induced biotoxicity of core-shell ZnSe/CdS QDs on cancer cell lines HEK-29, MCF-7 and EAC cells were treated with 10µg/ml of ZnSe/CdS quantum dots, incubated for 3 hrs, then fixed with 4% para-formaldehyde, and viewed under microscope [Nikon 90i] at Magnification 20x.

Tumour regression

The potential role of ZnSe/CdS quantum dots was assessed by testing its efficacy in Balb/c mice tumor model in terms

of tumor regression. Tumor regression results showed that ZnSe/CdS reduced the tumor burden negligibly when compared to control i.e. PBS. For simultaneous imaging and therapeutic uses, novel smart multifunctional QDs capable of sensing the release of therapeutics by altering the fluorescence of the imaging modality have been reported[42] as shown in **Fig. 6 (a)**. Toxicological issues relating to QDs have always been contentious owing to the heavy metal property of cadmium that is known to be toxic in its free form (Cd^{2+}). But, they are semiconducting in nature too, that enhances their photo-physical properties and imparts excellent tunable characteristics [**43**].

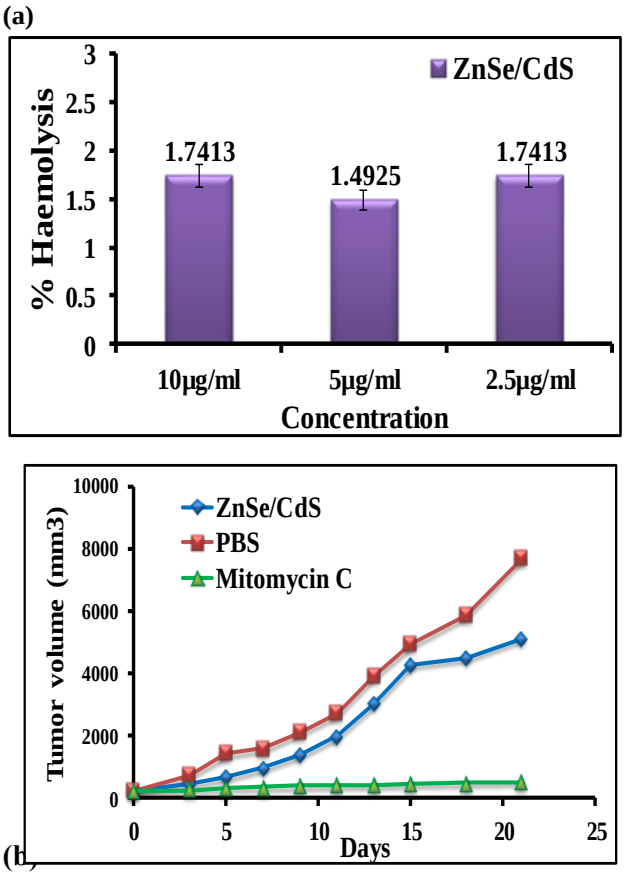

Fig. 6 (a) Effect of various ZnSe/CdS QDs concentrations on haemolysis post 2 hours incubation (b) Tumour regression by ZnSe/CdS QDs. Slight reduction in tumor burden was observed when compared to control (PBS).

Further, zinc selenide is reported to be potentially hazardous for neurological and genitourinary toxicity that further hinders the application of QDs to human subjects considerably. Indeed, in vivo toxicity is likely to be a key factor to determine whether QD imaging probes would be approved for human clinical use or not? Despite these limitations, QDs have been applied to cells and small animals as drug carriers, serving as an outstanding discovery tool for drug screening and validation and as prototype materials for drug carrier engineering. Su *et al.* [**44**] have also demonstrated that after the surface passivation with CdS and ZnSe shell, the cytotoxicity of the QDs were significantly suppressed. CdSe QDs are highly toxic to cultured cells for extended periods of time, but QDs with a stable polymer coating are not likely to be toxic to cells and animals. Paradoxically, ZnSe/CdS have shown negligible effects in in vivo studies done by Ballou and co-workers, thereby confirming the nontoxic nature of stable protected QDs. The effect of ZnSe/CdS QDs on tumour reduction was assessed in terms of the tumour volume over a period of 21 days **Fig. 7**. Approximately, 35% tumour regression was observed with the QDs as compared to placebo. The positive control mice exhibited a 93% reduction in of tumour volume. The reduction was not very significant in case of ZnSe/CdS. However, the tumour regression data post 21 days of injection clearly indicates that the QDs not only have a diagnostic value but also a therapeutic potential.

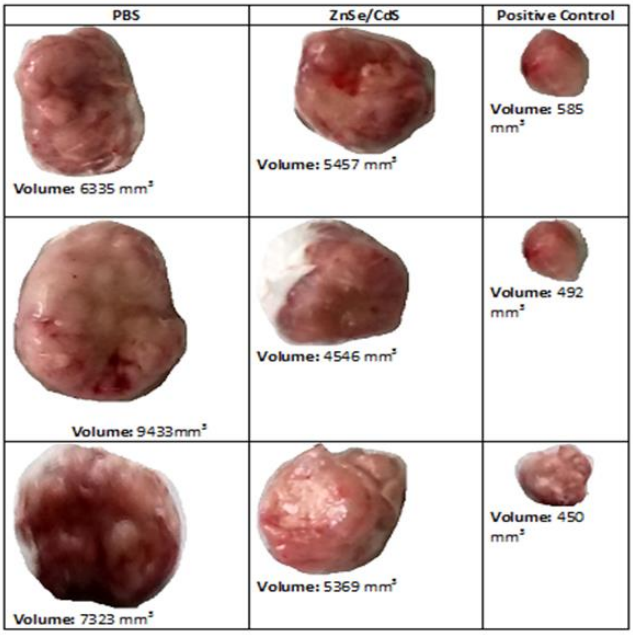

Fig. 7. Approximately, 34% Tumor Regression observed by ZnSe/CdS QDs, and 93% observed by Mitomycin C (Positive control) with respect to placebo (PBS).

Conclusion

Using 1, 2, 3-cycloocteno selenadiazole as a selenium precursor 1:1 CdS/CdSe, ZnSe/CdS and ZnSe/CdSe core shell QDs were successfully synthesized with tunable absorption and emission wavelengths. Among C6 and C8-SDZ, C6-SDZ was proved to be a successful precursor of selenium for synthesis of good quality ZnSe/CdS Core-shell QDs. It was observed that, thickness of shell layer increases with time and thus absorption value in the UV-visible spectra. Highly monodisperse and stable core shell QDs exhibited zinc blende crystal structure even after over coating with shell in all cases. The excellent monodispersity and high photoluminescence stability of the ZnSe/CdS core shell QDs impelled to study for cytotoxicity. As-synthesized ZnSe/CdS QDs showed more cytotoxicity towards MCF-7 cell line. It is believed that being hydrophobic in nature their retention time in a given cell line will be for a longer time thus causing greater damage. The prime challenge of drug delivery is to maintain an effective concentration of the drug in the targeted tissue while preventing toxicity. Another promising area of research is multifunctional nanoparticles that simultaneously deliver therapeutics and diagnostics or “theranostics". Drug delivery vehicles may be conjugated

to quantum dots or other nanoparticle probes to augment the treatment and monitor the tumors progression as the QDs are stable enough to be in the cells over a long period.

Acknowledgements

We are thankful to vice chancellor of DIAT (DU) for JRF/SRF to SB and AK. PKK thanks to DST, Govt. of India for research grant through project no. SR/S1/PC-39/2010s.

Reference

1. (a) Colvin, V. L.; Schlamp,M. C. and Alivisatos, A. P.;*Nature*, **1994**, *370, 354*. **DOI**:10.1038/370354a0
(b) Chen, X.;Samia, A. C. S.; Lou,Y. and Burda, C.;*J. Am. Chem.Soc.*, **2005**, *127, 4372*. **DOI:**10.1021/ja0458219
(c) Kudera, S.;Zanella, M.;Giannini, C.; Rizzo, A.; Li,Y. and Gigli, G.;*Adv. Mater.*, **2007**, *19, 548*. **DOI:** 10.1002/adma.200601015.
2. (a) Medintz, I. L.; Uyeda, H. T.; Goldman,E. R. and Mattoussi, H.;*Nat. Mater.***2005**, *4, 435*. **DOI:**10.1038/nmat1390
(b) Bowers, M. J.; Bride,J. R. Mc and Rosenthal, S. J.;*J. Am. Chem.Soc.*, **2005**, *127, 15378*. **DOI:**10.1021/ja055470d
(c) Sukhanova, A., Even-Desrumeaux K.; Kisserli, A.; Tabary, T.;Reveil, B.;Millot, J.-M.;Chames, P.;Baty, D.;Artemyev, M.;Oleinikov, V.;Pluot, M.; Cohen,J.H.M. and Nabiev, I.;*Nanomedicine: Nanotechnology, Biology, and Medicine*, **2012**, *8, 516*. **DOI:**:10.1016/j.nano.2011.07.007
(d)Wahab, R.; Khan,F.; Mishra,Y.K.; MusarratJ. and Al-Khedhairy, A. A.; *RSC Advances***2016**, 6, 32328-32339. **DOI:** 10.1039/C6RA05297E,
(e) Wahab, R.;Khan, F.; Yang, Y. B.; Hwang, I. H.; Shin, H.-S.; Ahmad, J.; Dwivedi, S.; Khan, S. T.; Siddiqui, M. A.; Saquib, Q.; Musarrat, J.; Al-Khedhairy, A. A.; Mishra, Y. K. and Ali, B. A.; RSC Advances 6, 2016, 26111-26120; **DOI:** 10.1039/C5RA25668B
(f)Dwivedi, S.; Wahab , R.; Khan, F.; Mishra, Y. K.; Musarrat, J. and Al-Khedhairy A. A. PLoS ONE **2014**, 9, e111289; **DOI:**10.1371/journal.pone.0111289
(g) Papavlassopoulos, H.; Mishra,Y. K.; Kaps, S.; Paulowicz, I.; Abdelaziz, R.; Elbahri,M. ; Maser, E.; Adelung, R. and Röhl,C.PLoS ONE 9, 2014,e84983, **DOI:**10.1371/journal.pone.0084983.
3. (a) Goldman, E. R.; Clapp, A. R.; Anderson, G. P.; Uyeda, H. T.; Mauro, J. M.;Medintz,I. L. and Mattoussi, H.;*Anal. Chem.*, **2004**, 76, 684–688. **DOI:**10.1021/ac035083r
(b) More, P.;Bharate, B. G.;Vishwanath,A. K. and Khanna, P. K.;*J. Lumin.*, **2010**, *130, 18*; **DOI:**10.1016/j.jlumin.2009.07.010
(c) Xia,Y. S. and Zhu, C. Q.;*Mater. Lett.*,**2008**, *62, 2103*. **DOI:**10.1016/j.matlet.2007.11.027
(d) Peng,Z. A.and Peng, X.;*J. Am. Chem. Soc*., **2002**, *124, 3343*. **DOI:**10.1021/ja0173167
(e) Firth, A. V.; Haggata, S. W.;Khanna, P. K.; Williams, S. J.; Allen, J. W.; Magennis, S. W.; Samuel, D.W. and Cole-Hamilton, D. J.;*J. Lumines.*,**2004**, *163, 109*. **DOI:**10.1016/j.jlumin.2004.02.004
4. Bang, J.; Yang, H. and Holloway, P. H., *Nanotechnology* **2006**, *17, 973–978*. **DOI**:10.1088/0957-4484/17/4/022
5. Bera, D.; Qian, L.; Tseng,T.-K. and Holloway,H. P.; *Materials***2010**, *3, 2260-2345*. **DOI**: 10.3390/ma3042260
6. (i) Colvin, V.L.; Goldstein, A. N.;Alivisatos,A.P. *J. Am. Chem. Soc.***1992**, *114, 5221–5230*. **DOI:**10.1021/ja00039a038
(ii) Dabbousi, B.O.; Murray, C. B.;Rubner,M.F. and Bawendi, M. G.;*Chem. Mater.***1994**, *6, 216–219*. **DOI:**10.1021/cm00038a020
7. Chen, X.B.; Lou, Y.B.;Samia, A.C.;Burda, C.;*Nano Lett.***2003**, *3, 799–803*. **DOI:**10.1021/nl034243b
8. Ivanov, S. A.;Priyatinaski, A.; Nanda, J.;Tretiak, S.;Zavadil, K. R.;Vallace, W. O.;Werder,D. and Klimov, V. I.;*J.Am. Chem. Soc.***2007**, 129, 11708-11719. **DOI:**10.1021/ja068351m
9. Kasakarage, H.; Kirsanova, N. N.; Nemchinov, M.; Schmall, A.; El-Khoury, N.; Tarnovsky,P. Z. and Zamkov, A. N.;*J. Am. Chem. Soc.*,**2009**,131,1328. **DOI:**10.1021/ja8082895
10. Dorfs, D.; Salant, A.; Popov,I. and Banin, U.;*Small*, **2008**, *4, 1319*. **DOI:**10.1002/smll.200800084
11. Manuela, F.; Chaniotakis, N.;*Sensors* **2009**, *9, 7266–7286*. **DOI:**10.3390/s90907266
12. Baek, S.-W.; Shim, J.-H.; Seung, H.-M.; Lee, G.-S.; Hong, J.-P.; Lee K.-S. and Gun J.; ***Nanoscale*,2014,6,** 12524-12531; **DOI:** 10.1039/C4NR02472A.
13. Kim, S.; Fisher, B.;Eisler, H.;Bawendi, M.;*J. Am. Chem. Soc.*,**2003**, *125,11466*. **DOI:**10.1021/ja0361749
14. Zhang, W.; Chen, G.; Wang, J.; Ye, B.;Zhong, X.;*Inorg. Chem.*,**2009**, 48, 9723. **DOI:**10.1021/ic9010949
15. Park, E.;Dvoracek, C.; Lee, H. K.; Galloway, J. F.; Bhang, H. C.;Pomper, M. G.;Searson, P. C.;*Small*,**2011**, *7, 3106*. **DOI:**10.1002/smll.201190087
16. Yang, X.; Zhao, D.;leck, K. S.;Tiam, T. S.; Tang, Y.X.; Zhao, J.;Demir, H. V.; Sun and Wei,X. *Adv. Met.***2012**, *24, 4180–4185*. **DOI:**10.1002/adma.201104990
17. Reiss, P.;Bleuse, J.; and Pron, A.;*Nano Letters*,**2002,***7, 781-784*. **DOI:**10.1021/nl025596y
18. Nizamoglu,S. and Demir,H. V.; *J. App. Phys.***2009**, 105, 083112. **DOI:**10.1063/1.3109151
19. Sharma, M.; Kumar,S. and Pandey, O. P.*Digest J. of Nanomat. and Biostr*.**2008,***3, 189*.http://www.chalcogen.ro/Sharma-Manoj.pdf
20. Fei, X.;Hao, Y.;Guo, J.;Jia, G.;Xie, L.; Wei, F.; Li,Q. and Hou, S.*Int. J. Electrochem. Sci.*,**2014,***9, 3795 – 3801*. http://www.electrochemsci.org/list14.htm#issue9
21. Wang, M.; Jiang, J.; Shi, J.; and Guo,L.; *ACS Appl. Mater. Interfaces*, **2013,** 5 (10), 4021. **DOI:**10.1021/am400851q
22. Peng, X.; Manna, L.; Yang, W.; Wickham, J.;Scher, E.;Kadavanich,A. and Alivisatos, A. P.;*Nature*,**2000**, *404, 59–61*. **DOI:**10.1038/35003535
23. Li, M.; Zaman, M. B.;Bardelang, D.; Wu, X.; Wang, D.;Margeson, J. C.; Leek, D. M.;Ripmeester, J. A.;Ratcliffe, C. I.; Lin, Q.; Yang,B. and Yu, K.;*Chem. Commun.***2009**, *6807*, DOI: 10.1039/B913914A**.**
24. Roy, M. D.;Herzing, A. A.;Lacerda,S. H. D. P. and Becker, M. L.;*Chem. Commun.***2008**, *2106–2108*. **DOI:**10.1039/B805691A
25. (a) Parak, W. J.;Gerion, D.; Pellegrino, T.;Zanchet, D.;Micheel, C.; Williams, S. C.; Boudreau, R.;Gros, M. A. Le;Larabell, C. A.;Alivisatos, A. P.;**DOI:**10.1002/1521-4095(20020618)14:12<882::AID-ADMA882>3.0.CO;2-Y, (b) Bhanoth, S.; Kshirsagar, A. S.; Khanna, P.K.; Tyagi, A.; Verma A. K.; *Advances in Nanoparticles*,**2016,** 5, 1-8. **DOI:** 10.4236/anp.2016.51001.
26. Sreenu, B.; More, P. V.;Jadhav, A.; Khanna, P. K.;*RSC Adv.*,**2014,***4, 17526-17532*. **DOI:**10.1039/C4RA00676C
27. (a) Khanna, P. K.;Beri, R. K.; More,P. V. and Bharate, B. G.; *Curr. Appl. Phys*, **2010**, 10, 553. **DOI:**10.1016/j.cap.2009.07.019
(b) Khanna, P. K.; More, P. V.; Shewate,R. and Beri, R. K.;*Chem. Lett.*, **2009,**38, 676. **DOI:** doi.org/10.1246/cl.2009.676
(c) Khanna, P. K.; Gorte,R. M. and Gokhale, R.;*Mater. Lett.*, **2004**,58, 966. **DOI:**10.1016/j.matlet.2003.07.035
(d) Jadhav, A.; More,P. V. and Khanna,P. K.; ***RSC Adv.,2015,***5, *76733–76742*. **DOI:** 10.1039/C5RA14625A
28. (a) Meir, H. and Voigt, E. ;*Tetrahedron*, **1972**, *28, 187* .**DOI :**10.1016/0040-4020(72)80068-1

(b) Khanna,P. K. and Morley, C.P.;*J.Chem.Res (S),***1995**, 64. (c) Khanna,P. K. and Morley, C. P.; *J. Organomet. Chem.,***1993,***109, 450.*
DOI:10.1016/0022-328X(93)80145-2.
29. Xia, D. A.;Lun, D.; Jin, X. W.; Li-Ping, Y.; Bo-Rui, Z.; Zhao,R. G. and Gang, Q. G.;*Chin. Phys. Lett,***2006**, *23(5),1317*.
DOI: http://dx.doi.org/10.1088/0256-307X/23/5/070
30. D.-A. Xia, D. Lun, X. W.-Jin, Y. Li-Ping, Z. Bo-Rui, R. G.Zhao and Q. G. Gang, Chin. Phys. Lett, 2006, 23(5),1317
DOI: 10.1088/0256
31. Verma, A. K.; Sachin, K.; Saxena, A. and Bohidar,H. B.; *Current Pharmaceutical Biotechnology*. **2005,***6,121-130*.
DOI: 10.2174/1389201053642349
32. Kumar, P. ;Meena, R.;Paulraj, R.;Chanchal, A.;Verma,A. K. and Bohidar, H. B.*Colloids and Surfaces B: Biointerfaces***2012,***91, 34.*
.**DOI:**10.1016/j.colsurfb.2011.10.034
33. Verma,A. K. and Sachin, K.;*Current Drug Delivery,***2008,***5, 120-126.*
DOI:10.2174/156720108783954806
34. Verma, A. K.;Chanchal, A.;ChutanI K.; *Int. J. of Nanotechnology*,**2012,***9,872-886*.
DOI: 10.1504/IJNT.2012.049452
35. Sharma, R.K.;Kedarnath, G.; Jain, V. K.;Wadawale, A.;Nalliath, M.;Pillaiand,C. G. S. and Vishwanadh B. *Dalton Trans.*,**2010,***39, 8779–8787;*
DOI: 10.1039/C0DT00263A
36. Dzhagan, V. M.;Valakh, M. Y.;Raevskaya, A. E.;Stroyuk, A. L.;Kuchmiy, S. Y.; Zahn, D. R. T.;*Nanotechnology*, **2007,***18, 285701.*
DOI: 10.1088/0957-4484/18/28/28570
1ii) Tschirner, N.; Lange, H.;Schliwa, A.; Biermann, A.; Thomsen, C.; Lambert, K.; Gomes, R.; Hens, Z.;*Chem. Mater.***2012,***24, 311−317.*
DOI:10.1021/cm202947n
(iii) Dzhagan, V. M.; Valakh, M. Y.; Milekhin, A. G.; Yeryukov, N. A.; Zahn, D. R.T.; Cassette, E.; Pons,T. and Dubertret, B.; *J. Phys. Chem. C***2013,** 117,18225−18233
DOI:10.1021/jp4046808
(iv) Nandakumar, P.;Vijayan, C.; Rajalakshmi, M.;Arora, A. K.; *Physica E* **2001,***11, 377–383.*
DOI:10.1016/S1386-9477(01)00157-6
37. Heiden, K.;Wiecinski, T. C.; Mangham, P. N.; Metz, A. N.; Nesbit, K. M.; Pedersen, D.;Hameras, J. A.; Heideman, R. J. ; Peterson, W.;*Environ Sci. tech.*,**2009,***43, 1605*.
DOI:10.1021/es801925c
38. Parak, W. J.; Boudreau, R.;*Adv Mater.***2002,***14, 882.*
DOI:10.1002/1521-4095(20020618)14:12<882::AID-ADMA882>3.0.CO;2-Y.
39. Beyersmann, D.;Hechtenberg, S.;*ToxicolApplPharmacol.***1997,***144, 247–261.*
DOI:10.1006/taap.1997.8125
40. Bruchez, M.;Moronne, M.; Gin, P.; Weiss, S.;Alivisatos, A. P.;*Science*. **1998,***281*.
DOI: 10.1126/science.281.5385.2013
41. Rikans, L. E.;Yamano, T. J.;*Journal of Biochemical and Molecular Toxicology*,**2000,***14, 110–117.*
DOI:10.1002/(SICI)1099-0461(2000)14:2<110::AID-JBT7>3.0.CO;2-J
42. Sanwlani, S.; Rawat, K.; Pal, M.; Bohidar, H. B.;Verma, A. K.;*J. Nanopart. Res.***2014,** 16, 2382.
DOI:10.1007/s11051-014-2382-6
43. Smith, A. M.; Dave, S.;Nie, S. M.; True, L.; Gao, X. H.; *Expert Rev MolDiagn***2006,** 6, 231.
DOI:10.1586/14737159.6.2.231
44. Gao, X. H.; Cui, Y. Y.;Levenson, R. M.; Chung, L.W.;Nie, S.; *Nat Biotechnol***2004,** 22, 969-976.
DOI:10.1038/nbt994
45. Su, Y.; He, Y.; Lu, H.; Sai, L.; Li, Q.; Li, W.; Wang, L.; Shen, P.; Huang, Q.; Fan, C.;*Biomaterials*, **2009,***30, 19-25.*
DOI:10.1016/j.biomaterials.2008.09.029

Supplementary information

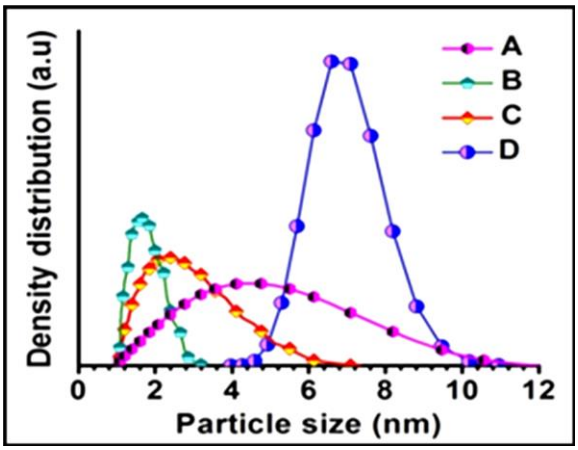

Fig. S1. Particle sizes of A) CdS/CdSe, B) ZnSe/CdS, C) ZnSe/CdSe using C8 as precursor and D) ZnSe/CdS synthesized using C6 as precursor.as-synthesized core-shell nanoparticles.

Table S1. The calculated FWHM from Raman spectra of the core-shell QDs near 400 cm^{-1} and its comparison with the particle size obtained from TEM.

Core-shell	FWHM (nm)	Particle size from TEM (nm)
A	25.00	4
B	18.00	6
C	24.61	5
D	26.30	3

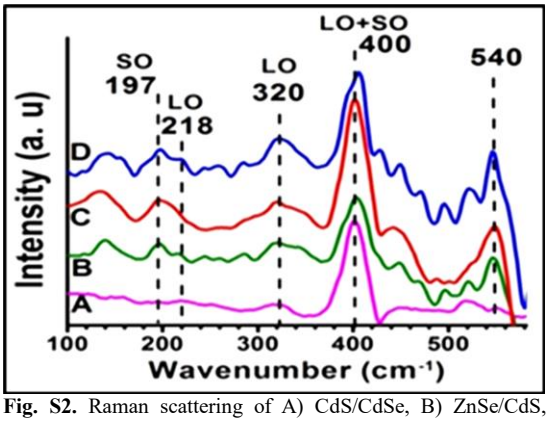

Fig. S2. Raman scattering of A) CdS/CdSe, B) ZnSe/CdS, C) ZnSe/CdSe using C8 as precursor and D) ZnSe/CdS synthesized using C6 as precursor.

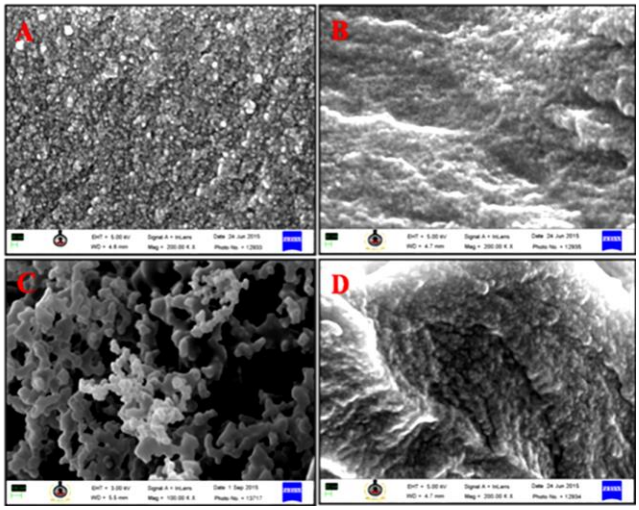

Fig. S3. SEM images of as-synthesized A) CdS/CdSe, B) ZnSe/CdS, C) ZnSe/CdSe using C8 as precursor and D) ZnSe/CdS synthesized using C6 as precursor (scale bar for images A, B, D is 30 nm and 100 nm for image C).